

PACS 42.15.Fr, 42.30.Ms, 42.30.Rx, 42.40.Eq, 42.40.My

Shack-hartmann wavefront sensor with holographic lenslet array for the aberration measurements in a speckle field

D.V. Podanchuk, V.N. Kurashov, V.P. Dan'ko, M.M. Kotov, N.S. Sutyagina

Optical Processing Laboratory, Faculty of Radiophysics,

Taras Shevchenko Kyiv National University, 64, Volodymyrska str., 01033 Kyiv, Ukraine

Abstract. The application of a Shack-Hartmann sensor with holographic lenslet array to the measurements of wavefront aberrations in a speckle field is offered. The main feature of the method is that the tested wave front can be compared with an arbitrary wavefront preliminary recorded in the holographic memory of the array. An iterative algorithm of the sensor work for measuring the variable speckled wavefronts is offered. The experimental results of measurements of the curvature of a spherical speckled wave are presented. The possibility to use the method proposed in the analysis of deformations of a rough surface is shown.

Keywords: sensor, speckle, holographic lenslet array, aberration measurement.

Manuscript received 29.01.08; accepted for publication 07.02.08; published online 31.03.08.

1. Introduction

The occurrence of phase and amplitude fluctuations in a tested beam, which appear as a result of the laser beam scattering by the randomly inhomogeneous medium, complicates or makes it impossible to carry out measurements by the wavefront sensors. Such a problem arises for aberration measurements of human eye using the laser illumination or, for example, for the precision monitoring of deformations of a rough surface by a wavefront sensor, etc. The laser illumination scattered by the surface gets to the wavefront sensor. Because of the microstructure of the eye retina or the rough surface, the speckle field considerably reducing the accuracy of the aberration determination arises. In this case, the random phase and amplitude modulation of the speckle field should be considered to be an obstacle when determining a large-phase distortion of the investigated wavefront. There are several ways to reduce this phenomenon [1, 2]. Most common are the methods of time averaging of speckles and the use of illuminations with different wavelengths. Each of these methods has its advantages and peculiarities but doesn't solve the problem of the aberration measurement accuracy increase *in corpore*. In this paper, the iterative algorithm of the work of a Shack-Hartmann wavefront sensor with holographic lenslet array is proposed for the wavefront aberration measurement in the presence of a speckle field [3].

2. Principles of the method

The Shack-Hartmann wavefront sensor belongs to the group of sensors that measure the local slopes of a wavefront and determine the phase of an optical wave by the discrete set of its first derivatives [4]. The investigated wavefront is directed to the lenslet array that forms a hartmannogram in the focal plane, whose image is recorded by a CCD-photodetector. The displacements of hartmannogram spots in relation to the corresponding lenslet optical axes are proportional to the wavefront slope averaged by each subaperture. The centers of spots are considered to be the centroids:

$$x = \frac{\sum_{i,j} x_{ij} I_{ij}}{\sum_{i,j} I_{ij}}; \quad y = \frac{\sum_{i,j} y_{ij} I_{ij}}{\sum_{i,j} I_{ij}}; \quad (1)$$

where I_{ij} is the intensity in the corresponding pixel; x_{ij} , y_{ij} are its coordinates; the summation being made over all pixels from the subaperture that belongs to the current lenslet. The wavefront shape reconstruction from the experimentally determined local slopes is made by the modal method, in which the wavefront phase is represented as the expansion in basis functions, the so-called modes. Generally, the basis of Zernike polynomials is used, since they describe standard aberrations [5].

Actually, the usual Shack-Hartmann sensor with a refractive lenslet array estimates the tested wavefront shape from its deviation from a plane wave. The abilities of modern holography allow creating a more universal wavefront sensor with comprehensive facilities [6, 7]. The basic difference of its work from the classic analog is the ability to compare the tested wavefront with an arbitrarily shaped wavefront which is recorded in the holographic memory of a lenslet array. Thus, an iterative algorithm of the sensor work on this basis will be developed for investigating the time-varying wave fronts distorted by speckles. At the first stage, the initial state of a speckled wavefront is recorded into the memory of a holographic lenslet array. The sensor will register the tested wavefront deflection from the initial stage. When the limit of the measurement range defined by the wavefront distortion degree is reached, the next holographic lenslet array is recorded, and so on. The whole dynamics of changing the tested wavefront shape can be defined by the sequential summation of the local slopes determined for every subaperture on different stages of the iterative process. Hereby, the value of local slope that can be measured for n iterations is determined as

$$\left(\frac{\partial\Phi}{\partial x}\right)_n = \sum_{m=1}^n \frac{\Delta x_m}{f},$$

$$\left(\frac{\partial\Phi}{\partial y}\right)_n = \sum_{m=1}^n \frac{\Delta y_m}{f}, \quad (2)$$

where Φ is the phase of the investigated wavefront, Δx_m and Δy_m are the maximal displacements of a focused spot that can be detected by the sensor for the m -th iteration, and f is the focal length of the lenslet array. Thus, the iterative algorithm of recording the holographic lenslet array and measuring the aberrations with the compensation of distortions for sequential stages of a speckled wavefront is realized. It's obvious that the

extension of the range of speckled wavefront measurements depends on the number of iterations.

3. Experimental setup

For the experimental verification of the iterative method of the holographic Shack-Hartmann wavefront sensor work, the laboratory setup was engineered; its optical scheme being shown on Fig. 1. A laser beam ($\lambda = 0.63 \mu\text{m}$) is divided into two beams by beam splitter BS1. One beam (the higher beam on the scheme) forms the reference wave for the holographic lenslet array recording. This beam passes through refractive lenslet array LA and, by means of beam delivery system L1–L2 and mirrors M1 and M5, is directed to the holographic plate at an angle of about 10° . The diameter of the lenslet array lenses is 0.4 mm , and the focal length is 24 mm .

The beam which passed through BS1 forms the object and the tested waves for the recording and reconstruction of holograms. The beam that is reflected from M2 and M4 mirrors forms the reference plane wave. The tested spherical wavefront is formed by the optical system of L3 and L4 lenses. The curvature of this beam can be changed by the micro-objective L3 shifting along the optical axis. On the outlet of the system, diffusive plate DP (ground glass) is placed. Statistical parameters of the speckle field are determined by a rough surface shape. The object wave also can be formed after the reflection from steel disc SD with rough surface that is placed instead of M4 mirror. With the L5–L6 lenses system, the surfaces of DP and reference mirror M4 are transposed to the recording plane of holograms. During the hologram recording, one of the beams – the tested one or the beam reflected from M2 mirror – is used as the object beam. The hologram recording is realized on holographic plates PFG-01. During the measurements, the holographic lenslet array is illuminated by the tested wave, so the reconstructed wave forms the hartmannogram on the surface of a photodetector CCD1 (768×576 , the pixel size is $10 \mu\text{m}$).

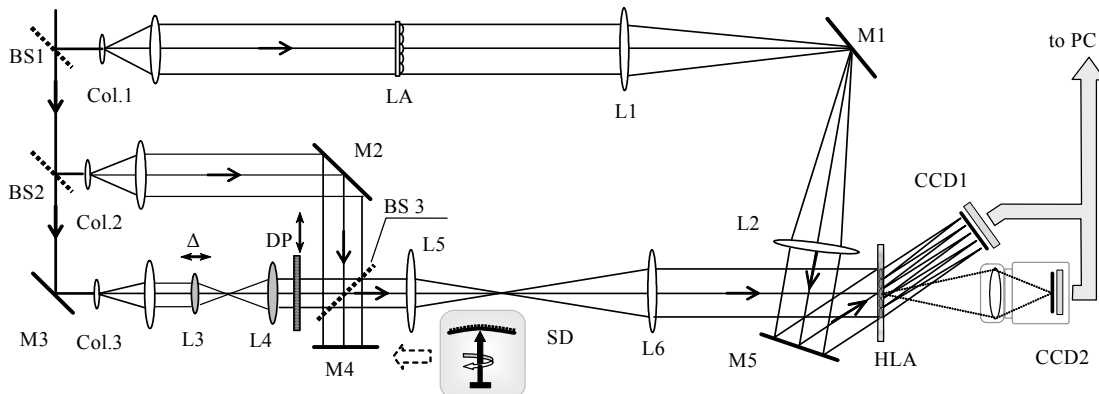


Fig. 1. Optical setup of a holographic Shack-Hartmann wavefront sensor: Col1-Col3 are collimators; LA/HLA is the refractive/holographic lenslet array; BS1–BS3 are beam-splitters; M1–M5 are mirrors; L1–L6 are lenses; DP is the ground glass; SD is the rough-surface steel disc; CCD1 and CCD2 are photodetectors.

To determine the wavefront local slopes, the array of 14×14 hartmannogram spots is used; it corresponds to the area of about 2 mm in diameter on the object plane. The tested wavefront curvature radius determination is realized by the value of the defocusing coefficient in the Zernike polynomial expansion of the wave front.

The veracity of the wavefront reconstruction by a wavefront sensor with holographic lenslet array can be reduced by the inaccuracy of the holograms positioning in the exposure place. This leads to the appearance of an additional aberration in the reconstructed wave front. To estimate these errors, the following experiments are performed. The tested wavefront shape on the stage of the HLA reconstruction is set to be the same, as it was during the hologram recording. Then the hologram is extracted from a holder and then mounted on that place again. During the data processing, the hartmannogram formed by a plane wave with the help of the refractive lenslet array is used as the reference, and the object hartmannogram is formed by the reference beam with the help of the holographic lenslet array. If the hologram is mounted precisely, the hartmannograms are identical, and, as a result of the reconstruction, we will obtain the plane wave. But in practice, there is some difference in hartmannograms that is revealed as the presence of some aberrations in the reconstructed wavefront. The aberration rate was quantitatively evaluated as the wavefront phase standard deviation from the plane wavefront phase throughout the tested aperture. The accuracy of the hologram positioning into the exposition place was visually controlled by the maximum fringe width of an interference image, which appears as a result of the interference between the wave reconstructed by the hologram and the object wave from the refractive array. In this case, the average standard deviation of the reconstructed wavefront phase was $\sim 0.05 \lambda$. This positioning method for holograms is used in the further work.

4. Results and discussion

At the first stage of the investigations, the influence of the speckle field on the results of wavefront measurements and reconstruction with a Shack-Hartmann sensor is estimated. Thereto, the holographic lenslet array is recorded with a plane reference wave formed by mirror M4. Thus, the diffractive analog of refractive LA is obtained. A clean or speckled tested wave front with the curvature that varied by the shifting of microobjective L3 is inputed to the sensor. The subimage of the speckle field and the fragment of corresponding noised hartmannogram of the plane wave front are depicted in Fig. 2a,b. As a diffuser, the one-side ground glass plate is used. Its surface is polished by a diamond paste with grains from 7 to 10 μm ; thus, the correlation radius of the speckle field in the hologram plane is $r_{\text{cor}} = 15 \mu\text{m}$. Figure 2b shows that the focused spots on the hartmannogram are splitted and noised. Therefore, the centroid estimation error increases and the

wavefront reconstruction error is revealed as the appearance of an additional aberration. The first ten coefficients of the Zernike polynomial expansion (up to the 3-rd order) for the reconstructed wave front are depicted in Fig. 2c (marks \square and \blacksquare represent the plane wavefront, \diamond and \blacklozenge represent the spherical wave). In case of a clean wave front (white marks), its shape is generally determined by defocusing aberration (coefficient C_3). But when the speckles appear (black marks), the defocus influence is reduced, because the rest expansion coefficients increase; thus, higher order aberrations “appear” in the reconstructed wave front, even when the plane wave is analyzed.

At the second stage, the application of the Shack-Hartmann sensor for spherical wavefront measurements in a speckle field is examined. The hologram of the refractive lenslet array with a plane reference beam reflected from M4 mirror is preliminarily registered. Then the obtained holographic lenslet array is reconstructed with the tested spherical wave. The dependence of the wavefront curvature on the micro-objective L3 shifting for the clean nonspeckled beam is shown in Fig. 3 (solid line a). To make these measurements, the ground glass is replaced by a transparent plate with the same thickness. Then the corresponding dependence is measured with a diffuser (marks b in Fig. 3). One can see that the curvature values for the speckled wave front obtained with the usual technique are significantly different from those for a clean beam without speckles.

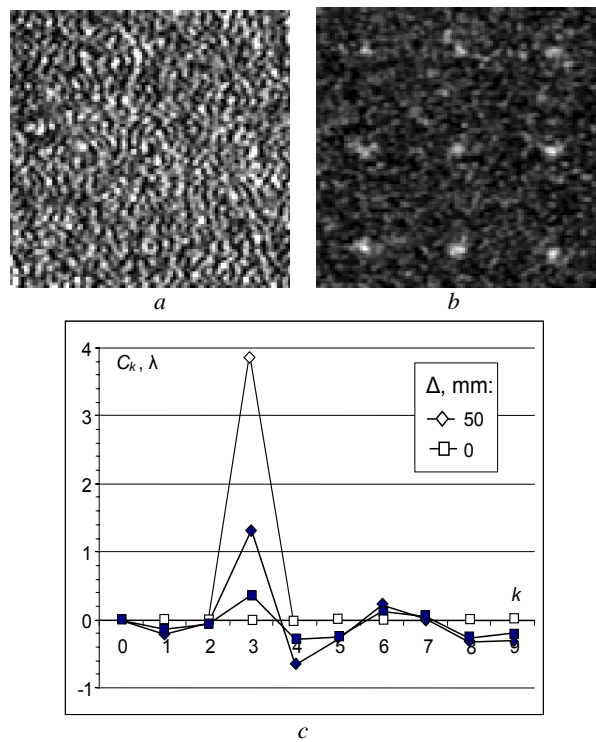


Fig. 2. a) Image of a speckle field with the correlation radius $r_{\text{cor}} = 15 \mu\text{m}$, b) corresponding noised hartmannogram, c) Zernike coefficients up to the 3-rd order for clean (white marks) and speckled (black marks) wave fronts.

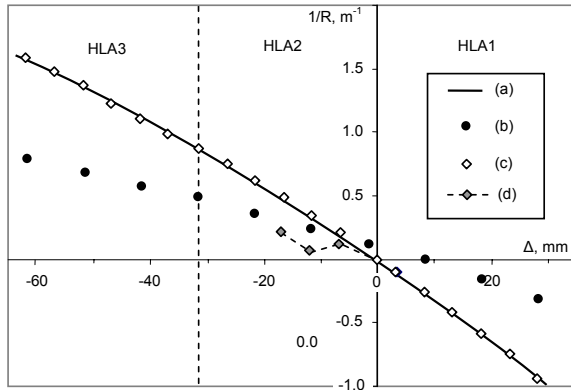


Fig. 3. Wavefront curvature measurements: a) in the absence of speckles; b) in the speckle field with a holographic copy of the usual lenslet array; c) in the speckle field with a holographic lenslet array and the iterative recording method; d) the error appearance because of overrunning the iteration range.

In Fig. 3 (marks c on the diagram), we also show results of the application of the iterative holographic lenslet array recording method to speckled wave front measurements (correlation radius $r_{cor} = 15 \mu\text{m}$). Three iterations were made when changing the wavefront curvature from 0.9 m^{-1} to $+1.6 \text{ m}^{-1}$: the first holographic array was recorded for a wavefront curvature of 0.93 m^{-1} , the second – for the plane wave, and the third for a curvature of $+0.86 \text{ m}^{-1}$. One can see that the usage of the proposed method considerably reduces the curvature measurement error down to several per cent. In our case, the iterative recording methods allow obtaining the reliable results when the wavefront curvature increases by 0.9 m^{-1} in comparison with the wavefront recorded in the holographic memory of the array. When the wavefront curvature overruns the measurement range of the holographic lenslet array, the rapid increase in the error is shown (dashed line d on the diagram).

The iterative recording algorithm was also applied to surface deformation measurements by means of the reflected beam analysis. Metallic disc SD with a diameter of 20 mm clamped around the periphery is used as a sample (see Fig. 1). During the measurements, it can be deformed with a flexure at the center controlled by the micrometer screw. Since the disc surface is rough, the speckles appear, when the probe beam is scattered after reflection. In this case, the application of a usual sensor is impossible because of the high noise level on the hartmannogram (Fig. 4a). But if the reflected speckled beam is used as the reference for the recording of the holographic lenslet array, then a noiseless hartmannogram with well-focused spots is formed in the focal plane of the lenslet array, while the hologram is being reconstructed (Fig. 4b). During the deformations of a sample, these spots are shifted proportionally to the local slopes of the surface, as it is in the absence of a speckle field; thus, the determination of a surface shape deviation from the initial shape of the sample becomes

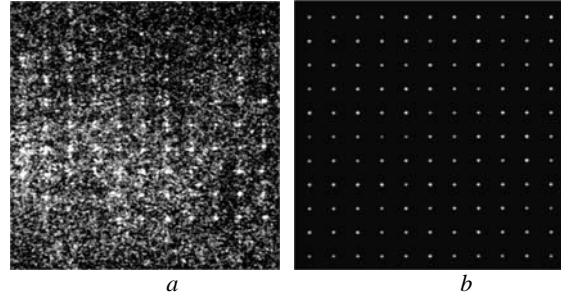


Fig. 4. Hartmannogram of the wave front reflected from the rough surface obtained with refractive (a) and holographic (b) LA.

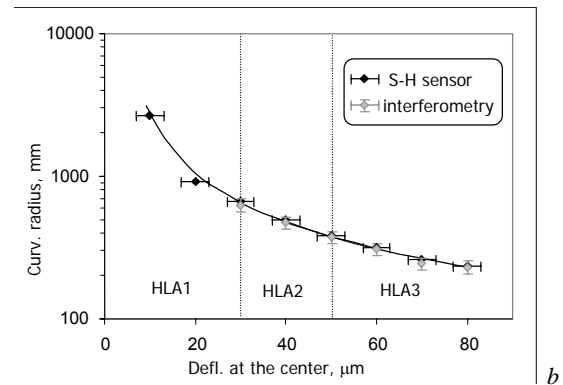
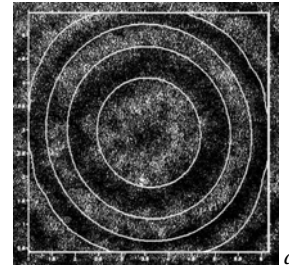


Fig. 5. a) Interferogram and a phase map of the wave front reflected from the rough surface with a 30- μm strain; b) measurements of the curvature radius of the sample shape.

possible. We sequentially recorded three HLAs with different states of the sample: with zero strain, and with deflections at the center of 30 and 50 μm .

The subsidiary control of the introduced surface deformation is realized by real-time holographic interferometric methods. For this, the hologram of an unstrained tested object is recorded; refractive lenslet array LA is removed from the beam to form the reference plane wave. The reconstruction of the hologram with the reference beam leads to the generation of a fringe pattern corresponding to the interference between waves reflected from the tested surface before and after the deformation. The fringe pattern is observed with a camera CCD2 focused on the plane of a hologram.

The interferogram obtained by the holographic interferometry method for a deflection of 30 μm at the center and superimposed with the phase map of the reconstructed wavefront is shown in Fig. 5a. One can see

that they are identical. However, the interferogram analysis is complicated because of the appearance of a speckle field. The greater the deformation, the greater the error of the interferogram processing. For example, when the deformation at the center is above 80 μm , the rings are almost indistinguishable against the speckled background. The sample's deformation was quantitatively evaluated by the surface curvature radius. Experimental values of the curvature radius are computed from the reconstructed Zernike coefficients and from the interference fringe radius. The results are given in Fig. 5b. The data obtained for different methods well coincide. The parts of the experimental curve obtained for different HLAs are uninterrupted, and it is more even in comparison with the curve for interferometric measurements.

5. Conclusion

The discussed iterative method of the holographic lenslet array recording advances the Shack-Hartmann wavefront sensor features. The possibility of its use for the measurement of aberrations in a speckle field by the holographic compensation of distortions for sequential states of the speckled wavefront is shown. The usage of a reversible material for the holographic lenslet array recording is expected to allow the realization of the Shack-Hartmann sensor, which easily accommodates to the dynamic changes of the wavefront. Such a sensor can find applications in optical metrology, e.g. for the real-time testing of a rough surface deformation.

References

1. A.V. Larichev, P.V. Ivanov, N.G. Iroshnikov, V.I. Shmalhauzen, Measurement of eye aberrations in a speckle field // *Quantum Electronics* **31**, p. 1108-1112 (2001).
2. V. Albanis, E.N. Ribak, Y. Carmon, Speckle reduction in wave-front sensing, In: *Adaptive Optics: Analysis and Methods*, Ed. B. Ellerbroek. Vancouver, Canada, Optical Society of America, 2007.
3. D.V. Podanchuk, V.P. Dan'ko, M.M. Kotov, N.S. Sutyagina, Iterative expansion of the measurement range of the Shack-Hartmann wavefront sensor // *Bulletin of the Kyiv National University, Series: Physics & Mathematics* **1**, p. 306-314 (2006).
4. G. Rousset, Wavefront sensing, In: *Adaptive Optics for Astronomy*, Eds. D. M. Alloin, J.-M. Mariotti. p. 116-137, Kluwer, Dordrecht, 1994.
5. J.Y. Wang and D.E. Silva, Wave-front interpretation with Zernike polynomials // *Appl. Opt.* **19**, p. 1510-1518 (1980).
6. J.Y. Son, D.V. Podanchuk, V.P. Danko, K.D. Kwak, Shack-Hartmann wavefront sensor with holographic memory // *Optical Engineering* **42**(11), p. 3389-3398 (2003).
7. D.V. Podanchuk, V.P. Dan'ko, M.M. Kotov, J.-Y. Son, Y.-J. Choi, Extended-range Shack-Hartmann wavefront sensor with nonlinear holographic lenslet array // *Optical Engineering* **45**(5), p. 53605 (2006).